Wojciech KRAJEWSKI

MINIATURIZATION OF MEDIUM VOLTAGE COMPACT SWITCHGEAR

ABSTRACT *The miniaturisation of compact switchgears leads to savings in materials and enables the appliances' price to be reduced. It is beneficial for both manufacturers and customers. Nevertheless, the saving in the materials used should not impinge on the product's quality. Some aspects of the miniaturization of 24 kV compact switchgear, produced by the Polish company ZPUE S.A., are presented in this paper. The R&D Department of the factory has proposed to remove some redundant elements and walls of the external switchgear casing. The possibility of a further reduction in the dimensions of this new switchgear casing is considered in the present paper. To this end the electric field distribution inside the switchgear is analysed. This analysis has been done with the Maxwell 3D (Ansys) software package, which employs the finite element method (FEM).*

Keywords: *compact switchgear, electric field, electric withstand, finite element method, miniaturization*
DOI: 10.5604/01.3001.0010.0035

1. INTRODUCTION

Material saving brings down the costs involved in manufacturing a product, which normally leads to a reduction in the product's price. Generally, the saving in materials also has an ecological benefit because it limits energy use and consequently diminishes the production of greenhouse gases. Therefore, material saving is essential for the manufacturer as well as for the customer, and is also very significant for global environmental protection. Nevertheless, economising on materials should not compromise the appliance's quality.

In the present paper, some aspects of the miniaturisation of a 24 kV compact switchgear produced by the Polish company ZPUE S.A. are considered. This switchgear consists of three load switches, an earthing switch, fuses, busbars and two feeder bays. SF_6 is used as the general insulation of this gas insulated switchgear (GIS).

Wojciech KRAJEWSKI, Ph.D., D.Sc., Assoc. Prof.
e-mail: w.krajewski@iel.waw.pl

Electrotechnical Institute,
ul. Pożaryskiego 28, 04-703 Warsaw, Poland

The R&D department of the factory proposed to dispose some redundant elements of the enclosure, especially some of the external walls and internal partitions. Additionally, the switchgear fuses are located outside the new enclosure as shown in Figure 1. This modification significantly reduces the switchgear's overall dimensions, its weight, and the materials needed for its manufacture. The previous version of this switchgear was shown in [1, 2].

The possibility of the miniaturization of internal switchgear devices, for further appliance modification, is analysed here. The question is whether the distances between the energized elements, as well as between the energized elements and the earthed ones, (of the above-mentioned devices) can be reduced without worsening the switchgear parameters imposed by the standard PN-EN 62271-200: 2012 [3].

Similar analysis has been already done in [2] for the load switch that is used in the switchgear under consideration. The results obtained indicated that this apparatus is oversized and its dimensions can be reduced.

The present paper can be treated as a continuation of the above-mentioned work by the author. The computational results of the electric field distributions near busbars as well as inside a feeder bay are presented here. This analysis has been done with the professional software package Maxwell 3D (Ansys) [4], which is based on the finite element method (FEM) [5].

2. BASIC TECHNICAL DATA OF THE SWITCHGEAR

A general view of the modified GIS and its equipment are shown in Figure 1a and 1b, respectively. The basic technical parameters of this switchgear are given in Table 1.

In the switchgear under consideration, SF_6 is used as the general insulation for the internal devices but the bushings are insulated with an epoxy resin.

The electric withstand of SF_6 is about 3 times greater than the electric withstand of air [6, 7], i.e. about 60 kV/cm (r.m.s.) in normal atmospheric conditions. Obviously, this value is greater for the increased gas pressure [7], equal to 125 kPa, (Tab. 1) in the switchgear under consideration. Therefore, 75 kV/cm can be assumed (for the above pressure) as the electric field strength of the sparkover in the homogeneous field

TABLE 1
Basic technical data of the switchgear

Nominal grid voltage	20 kV
Highest apparatus voltage	24 kV
Rated frequency	50 Hz
Rated power frequency withstand voltage	50 kV/60 kV
Rated lightning impulse withstand voltage 1.2/50 μs	125 kV/145 kV
General insulation	SF_6
SF_6 pressure	125 kPa (20°C)
Insulator material	epoxy resin

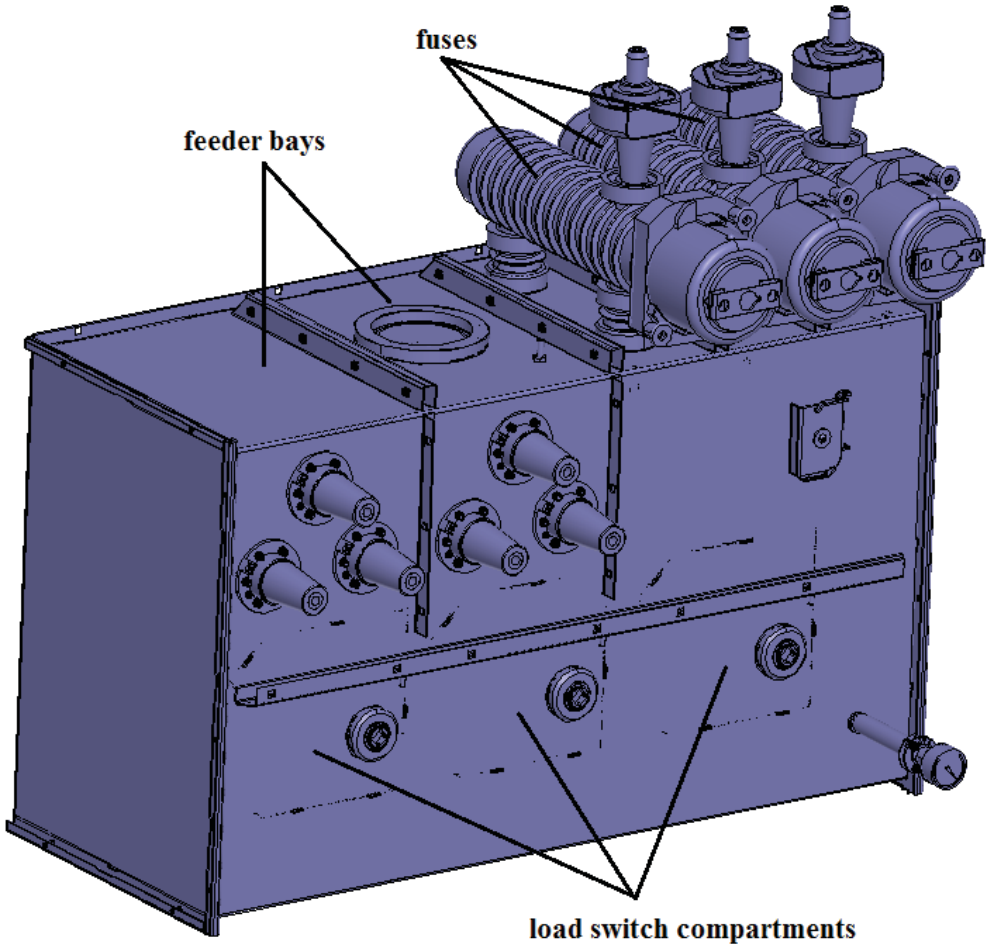

Fig. 1a. Modified 24 kV switchgear – general view

condition. In the case of a strongly inhomogeneous field, the above value (of the electric field strength) should be treated only as an inception value for partial discharges [6]. In such a situation, a sparkover does not occur.

The electric withstand of the epoxy resin is much greater than the withstand of SF_6 and is about 200 kV/cm. Nevertheless, the energized conductors of the bushings are located very close to the earthed metal casing. This can cause very high field strength on the surfaces of the resin insulators.

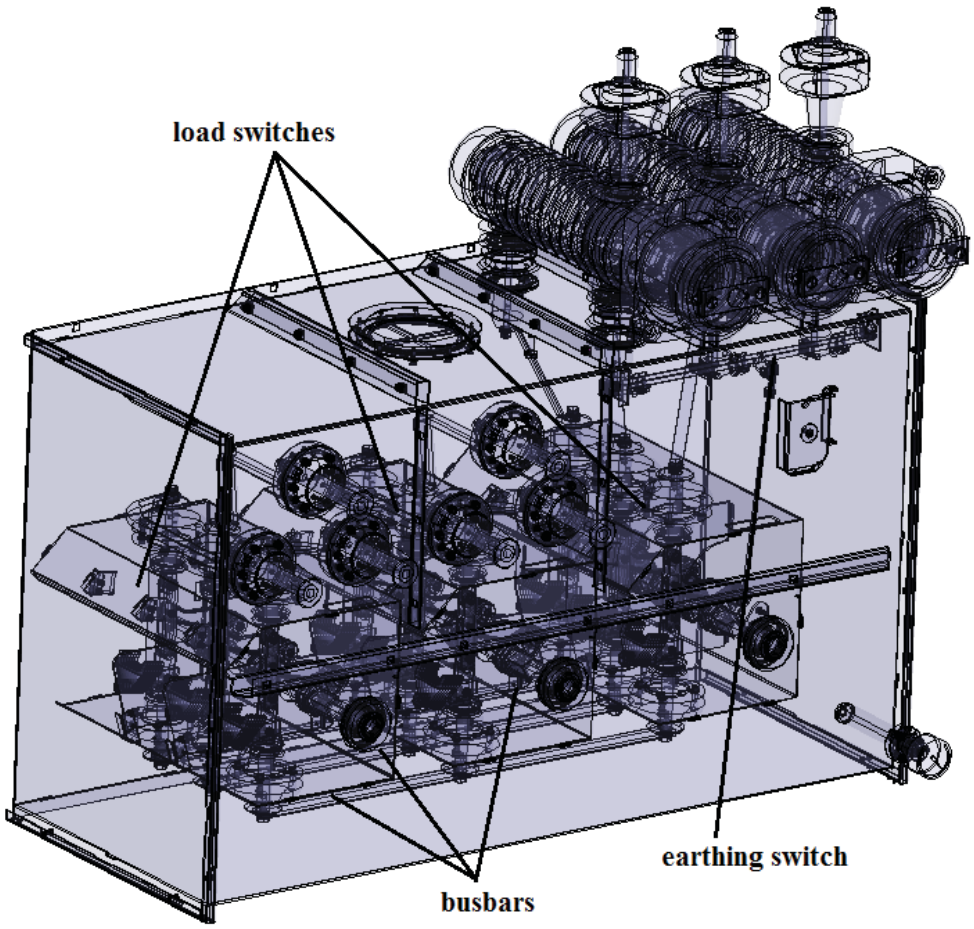

Fig. 1b. Modified 24 kV switchgear – equipment

3. DEVICES UNDER CONSIDERATION

As mentioned above, the electric field analysis (presented in the paper) concerns the feeder bay and busbar compartment. The feeder bay and the busbars are shown in Figures 3 and 4, respectively. In the switchgear under consideration, the feeder bays are connected with the busbars through the load switches which are shown in Figure 1b. The busbars are also connected with fuses that are located on the top of the enclosure. These fuses are used for the transformer's protection.

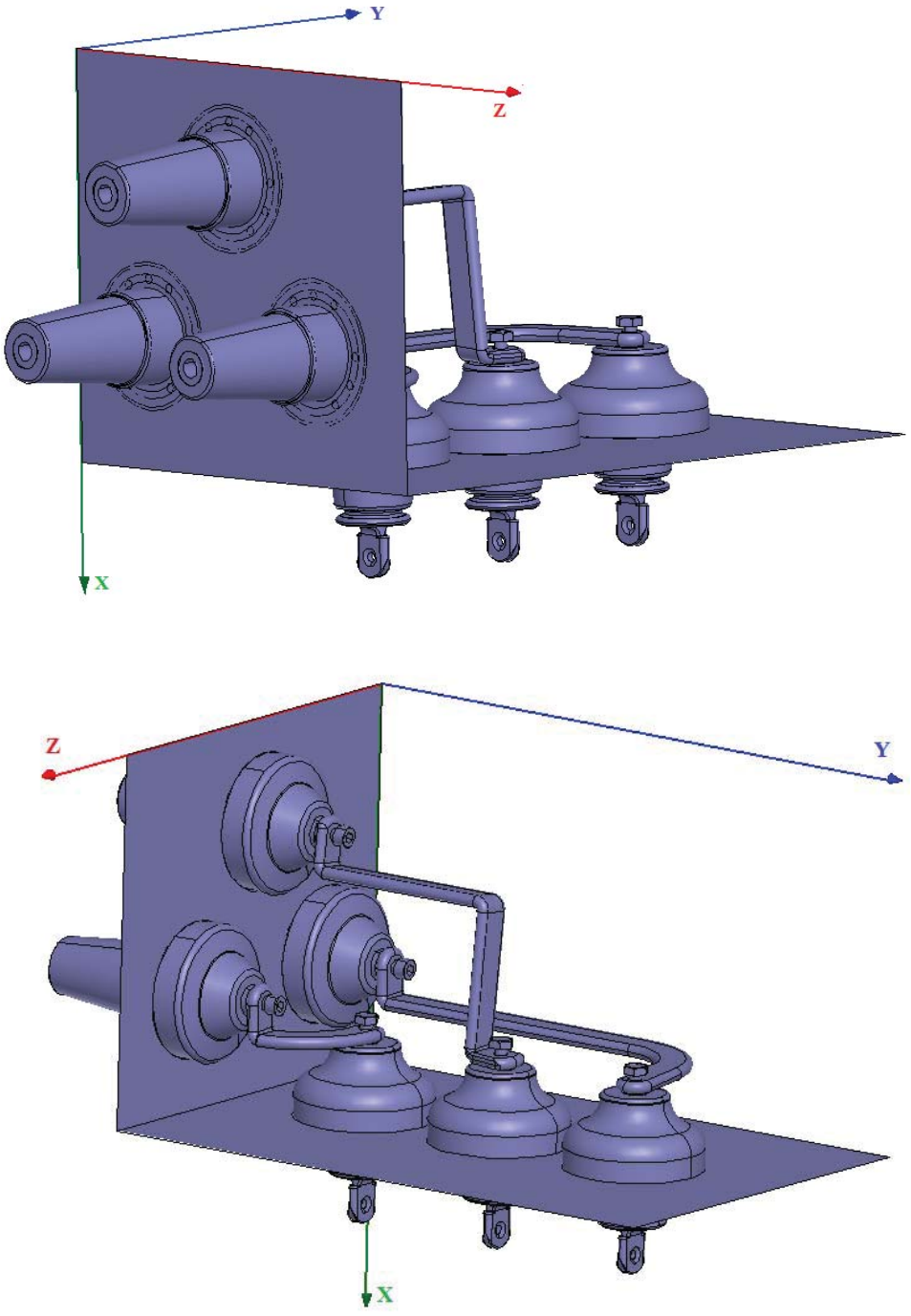

Fig. 2. Feeder bay

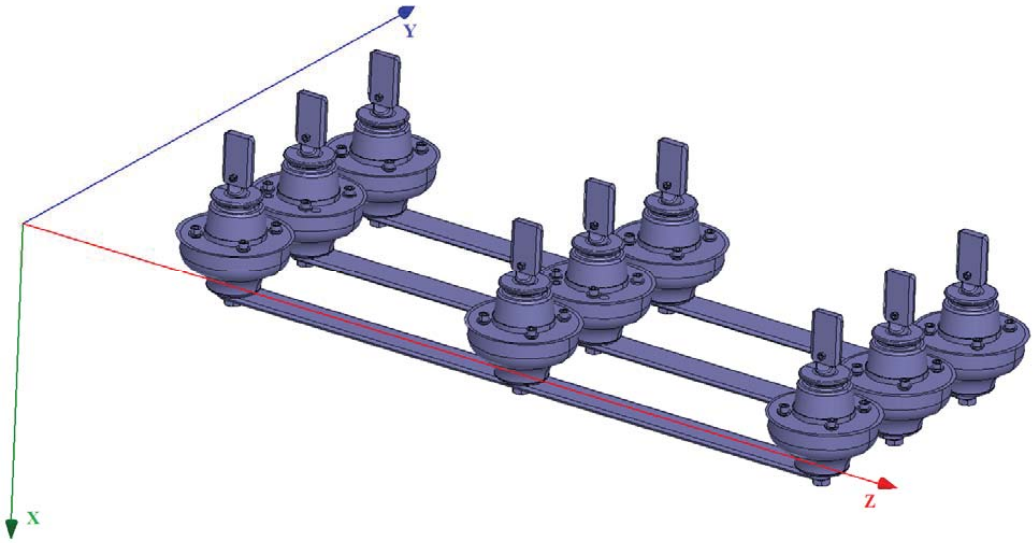

Fig. 3. Switchgear busbars

4. MATHEMATICAL FORMULATION OF THE PROBLEM AND THE NUMERICAL TECHNIQUE APPLIED

Precise mathematical modelling of the electric field inside switchgears requires a 3D approach because of the complex geometry of the problem. The field in question (produced by the energized elements) is affected by many earthed metal elements (the casing, partitions, supporting elements, screws, nuts, bolts, rivets, etc.) which can change the field distribution considerably. Such a problem can be solved only by the use of numerical techniques.

The finite element method (FEM), the boundary element method (BEM) [8], the charge simulation method (CSM) [9], and various combinations of these three techniques [10, 11] are most frequently used for the analysis of electric fields in power objects.

The BEM and CSM are very well suited to the modelling of open boundary problems, i.e. problems without boundary conditions. Therefore, these methods have been previously used for the analysis of the electric field distribution inside outdoor substations [11–16].

For the analysis of the electric field inside the compact GIS with a metal enclosure, the FEM looks more appropriate [2, 17]. The arguments for choosing this approach rest on the main advantages of the FEM, namely:

- Precise representation of a complex geometry,
- Simple inclusion of dissimilar material properties,

- Easy representation of the total solution,
- Simple extraction of local effects.

Therefore, the FEM has been employed in the investigations presented in this paper.

The boundary-value problem for the scalar electric potential is described by the 3D Laplace partial differential equation:

$$\nabla^2 \varphi = 0 \tag{1}$$

The appropriate boundary conditions are described below. Namely, on the surfaces Γ of conducting elements on which the electric potential, φ, is known, Dirichlet's boundary condition is applied:

$$\varphi\Big|_{\Gamma} = \overline{\varphi} \tag{2}$$

On the other hand, on the surfaces of conducting elements, Γ_C, where the electric potential is of an unknown value, the following boundary condition is introduced:

$$\varphi\Big|_{\Gamma_C} = \mathrm{C} \tag{3}$$

where C is a constant value. Such a condition appears on the boundary of a conducting element that is entirely surrounded by a dielectric environment. Because the constant C is of an unknown value, an additional equation has to be introduced to obtain a unique solution for the boundary-value problem. This equation results from Gauss's law and has the following form:

$$\iint_{\Gamma_C} \varepsilon \frac{\partial \varphi}{\partial n} d\Gamma = 0 \tag{4}$$

where ε is the electric permittivity of the surrounding dielectric.

The continuity condition on the interface Γ_I between dielectrics of different electric permittivities (e.g. the surface of the epoxy-resin element that is immersed in the gas) has to be taken into account as well. This condition is given below:

$$\varepsilon^{+} \frac{\partial \varphi}{\partial n}\Big|_{\Gamma_I^{+}} - \varepsilon^{-} \frac{\partial \varphi}{\partial n}\Big|_{\Gamma_I^{-}} = 0 \tag{5}$$

where ε^{+} and ε^{-} are the electric permittivities of the adjacent dielectric elements. After the solution of the boundary-value problem, the electric field strength is computed using the well-known formula:

$$\boldsymbol{E} = -\nabla \varphi \tag{6}$$

5. NUMERICAL MODELS OF THE DEVICES UNDER CONSIDERATION

In this section, the numerical models of the devices under consideration are presented. Approximations of these objects using finite elements are shown in Figures 4 and 5. Some inessential elements have been omitted from the numerical model used. It should be mentioned that the external part of the feeder bay is surrounded by a non-conductive subregion with a homogeneous Dirichlet boundary condition, which has facilitated the process of numerical computations without significantly worsening the accuracy of the computational results.

The computational results presented have thrown light on whether the insulation distances to earth and between the phases can be reduced to diminish the device's dimensions.

In accordance with [1] a voltage of 50 kV was applied to the conductors of the main circuit of the device under consideration. This is the withstand voltage (imposed by [1]) of the rated frequency for the 24 kV GIS.

In the first step, so called tests to earth were carried out, i.e. all the conductors of the main circuit were connected to a single phase supply of 50 kV and the remaining metal elements were earthed. In the consecutive computations, the insulation distances between the phases were checked. In this case, one of the main conductors was energised but the others were earthed.

The FEM approximation of the domains under consideration are shown in Figures 4 and 5.

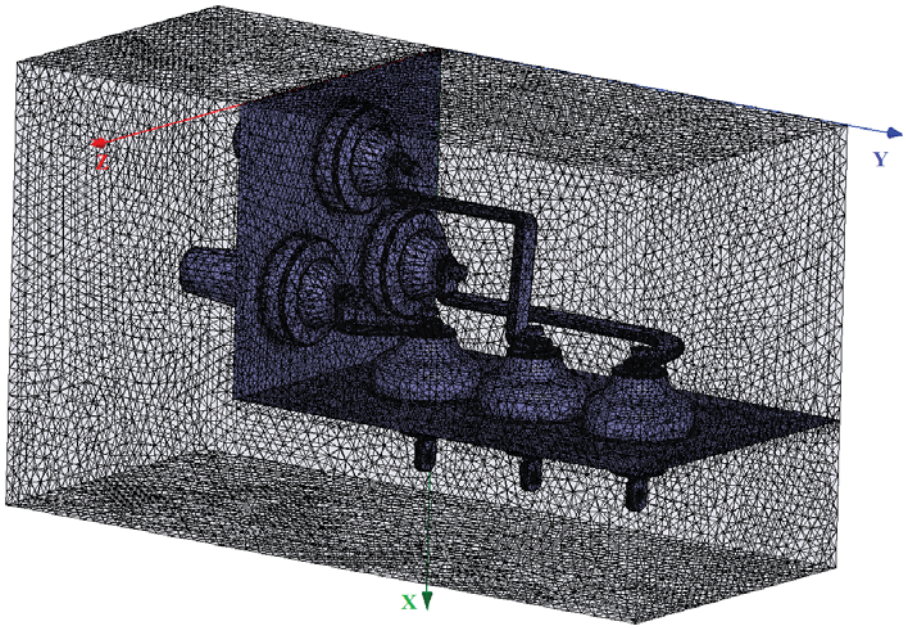

Fig. 4. Feeder bay and its approximation using finite elements

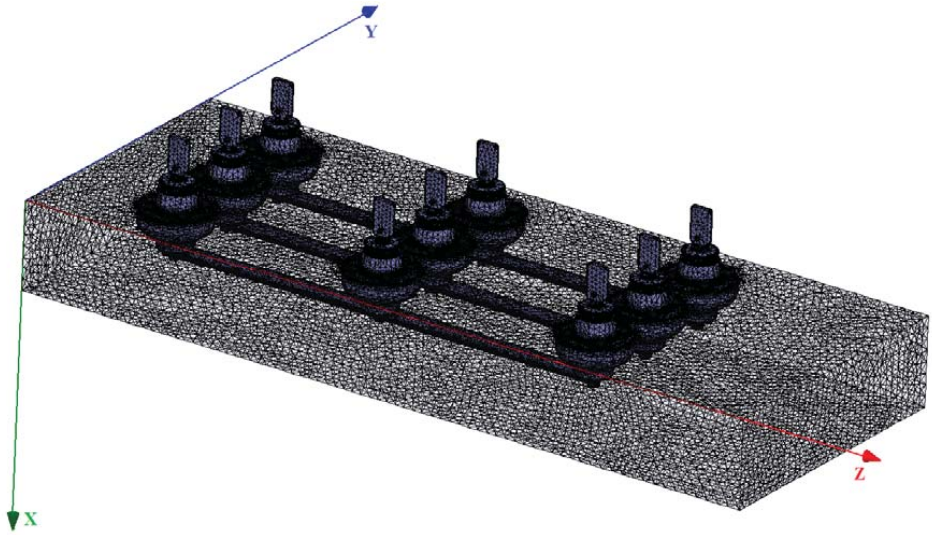

Fig. 5. Busbar compartment and its approximation using finite elements

6. COMPUTATIONAL RESULTS OF THE ELECTRIC FIELD DISTRIBUTION INSIDE THE FEEDER BAY

The numerical results of the electric field distribution inside one of the switchgear feeder bays are presented and discussed in this section.

The overall dimensions of the above switchgear compartment are: 300 mm in x direction, 500 mm in y direction, and 335 mm in z direction.

At the beginning, the computational results concerning the test to earth are presented. In this case, all the conductors of the main circuit were connected to a single phase supply as shown in Figure 6.

A vector map of the electric field in the domain in question is shown in Figure 7. This figure indicates that the significant values of the electric field strength appear near the energised conductors. Detailed electric field distribution maps in the regions with predicted high field strength are shown in Figures 8–11. The electric field strength on several flat vertical surfaces is shown in these figures, namely:

– on a plane ($y = 60$ mm) close to the heads of the horizontal insulators (Fig. 8),

– on planes ($y = 185$ mm and $y = 310$ mm) located between the vertical insulators (Figs. 9 and 10),

– on a plane ($y = 450$ mm) located between the vertical insulator and the casing (Fig. 11).

The electric field strength does not exceed 28 kV/m on these surfaces. This value is about 2.5 times smaller than the electric withstand of the gas insulation (SF_6 at a pressure of 125 kPa).

The electric field distributions at the cubicle's steel partitions with the bushings that pass them through are shown in Figure 12. The field distribution in this area is especially interesting from a practical point of view because the distance between the bushing conductor and the earthed metal partition is at its minimum value in this location, which implies that the electric field strength reaches the maximum value on these partitions. In this example, this value does not exceed 60 kV/m, which is over three times smaller than the electric withstand of the epoxy resin insulators.

To accomplish the electric field estimation in the feeder bay, the insulating distance between the phases should be tested as well. In this case, one of the main circuit conductors was energised (Fig. 13) but the remaining ones, as well as other metal elements, were earthed.

The vector map of the electric field strength in the feeder bay (for the above test) is shown in Figure 14. The electric field distributions on the planes where $y = 185$ mm and $y = 310$ mm are shown in Figures 15 and 16, respectively. The electric field strength does not exceed 21 kV/m on these surfaces, which is about 3.5 times smaller than the electric withstand of the SF_6 insulation.

The numerical analysis presented above indicates that the compartment under consideration is oversized and its dimensions can be significantly reduced.

The above computations have been done using a PC equipped with a 3.4 GHz Intel Core i7-2600K processor and 24 GB RAM. The total solution time (including the mesh generation, the calculation of algebraic equation coefficients and the solution of the algebraic equation system) was about 2 h.

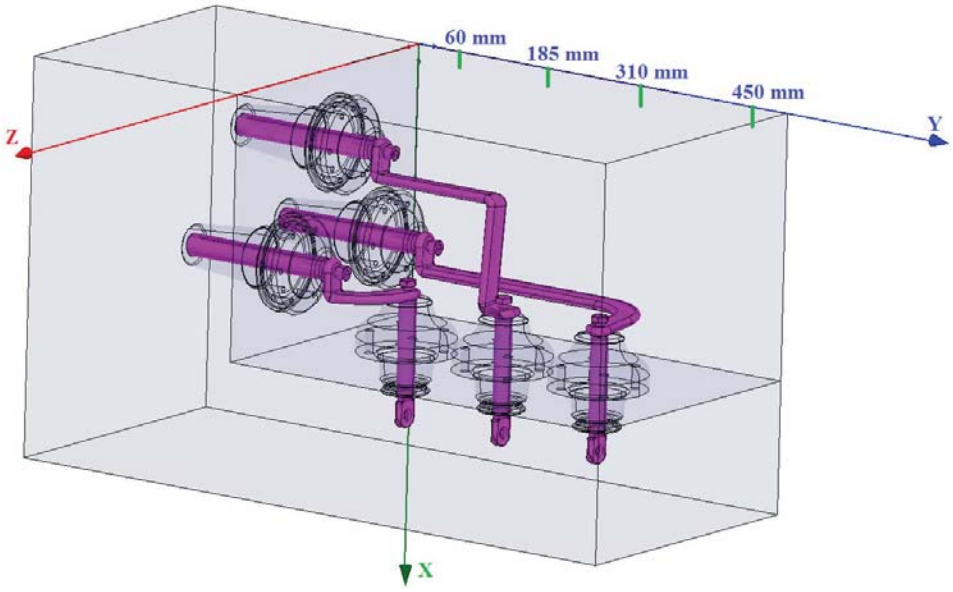

Fig. 6. Energised elements (magenta) in the feeder bay during the test to earth

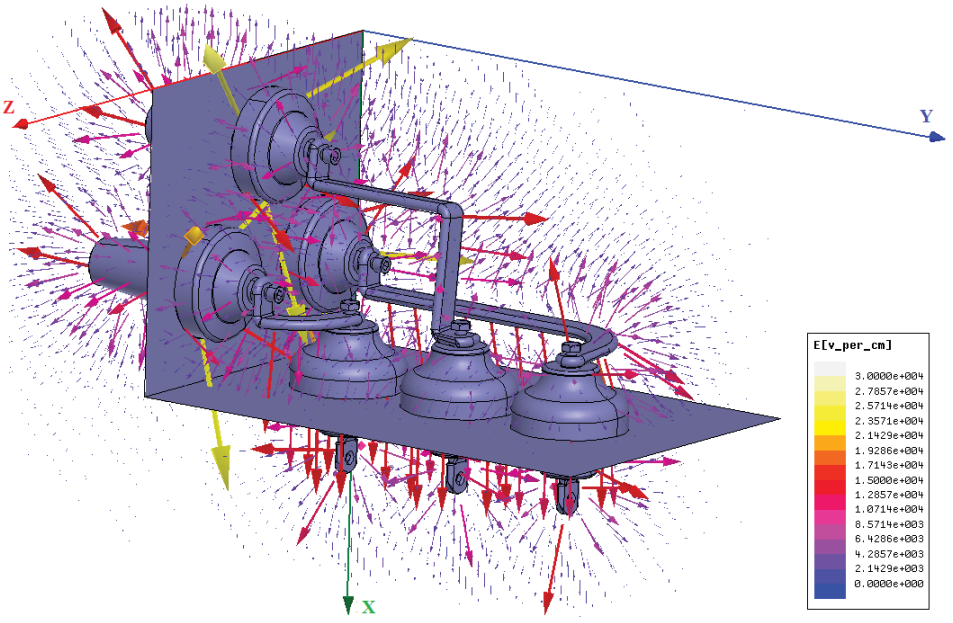

Fig. 7. Vector map of the electric field distribution in the feeder bay (test to earth conditions)

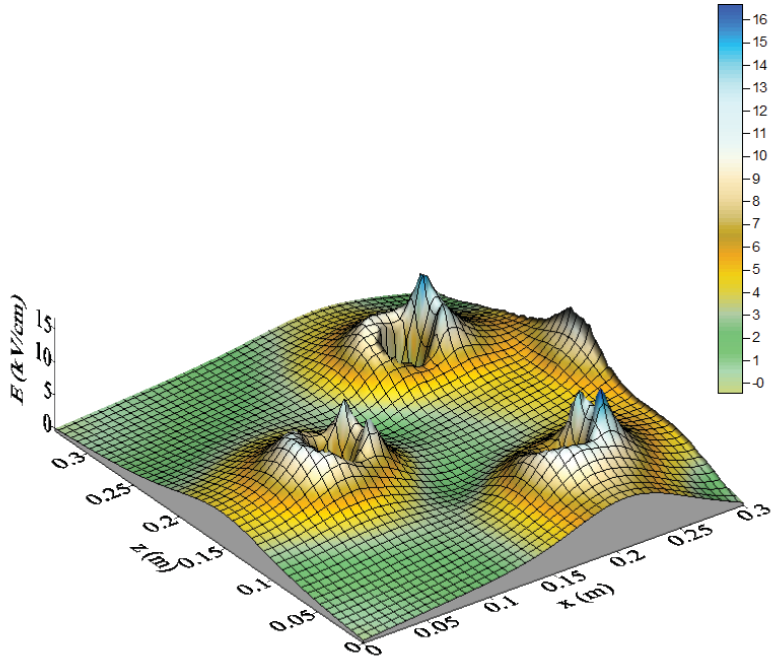

Fig. 8. Electric field distribution on the vertical plane (y = 60 mm) located near the heads of horizontal insulators in the feeder bay (test to earth conditions)

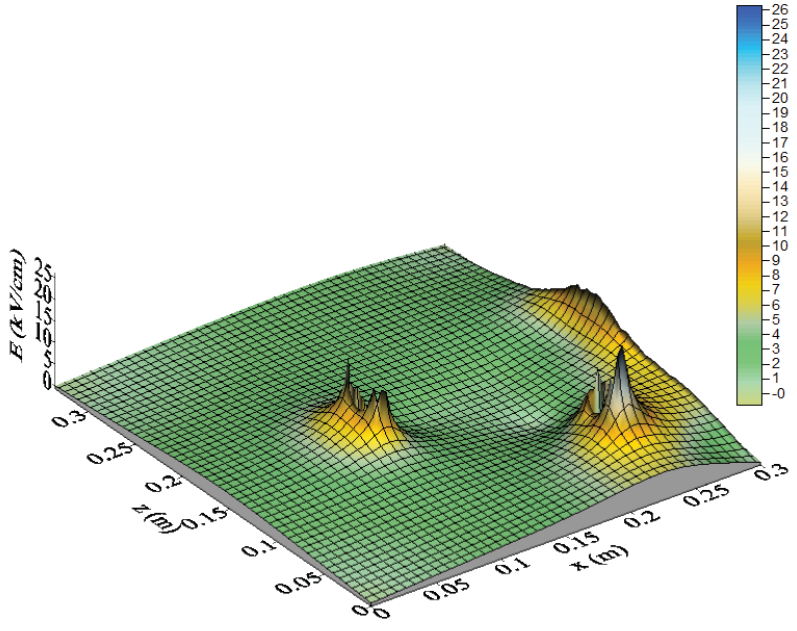

Fig. 9. Electric field distribution on the vertical plane (y = 185 mm) located between the vertical insulators of the feeder bay (test to earth conditions)

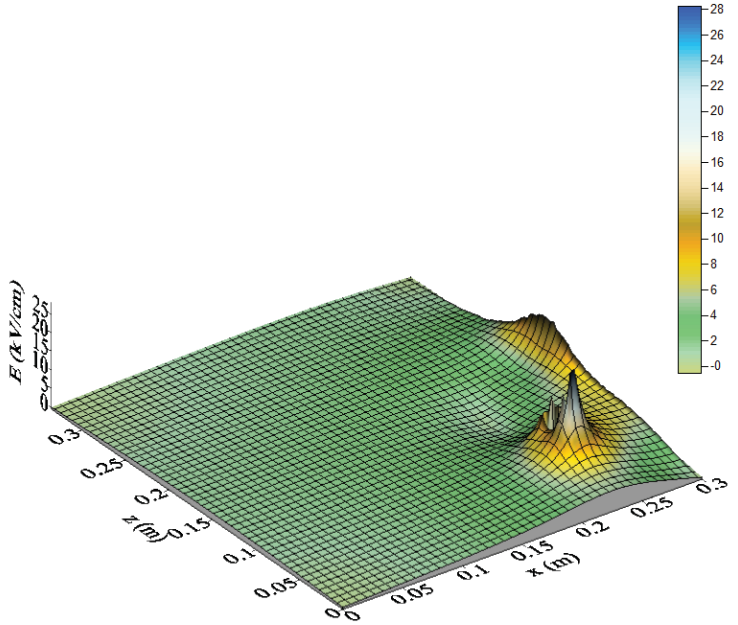

Fig. 10. Electric field distribution on the vertical plane (*y* = 310 mm) located between the vertical insulators of the feeder bay (test to earth conditions)

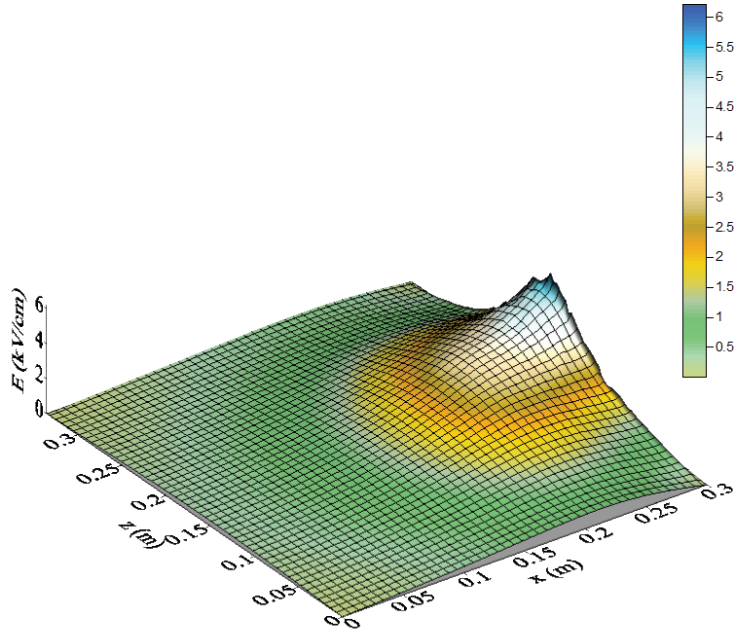

Fig. 11. Electric field distribution on the vertical plane (*y* = 450 mm) located between the insulator and the casing of the feeder bay (test to earth conditions)

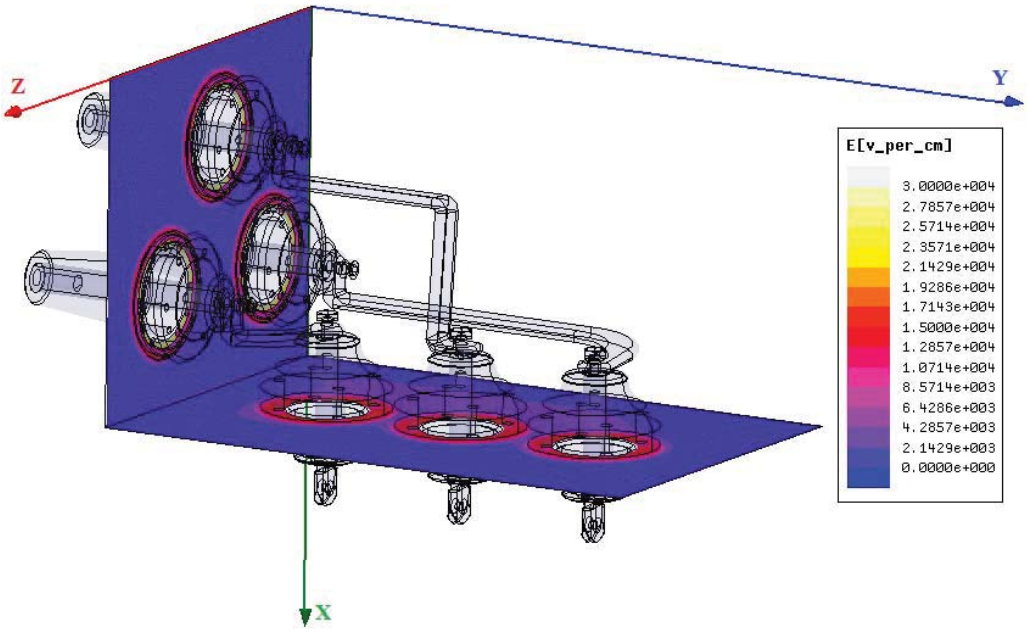

Fig. 12. Colour map of the electric field distribution around the bushings in the feeder bay (test to earth conditions)

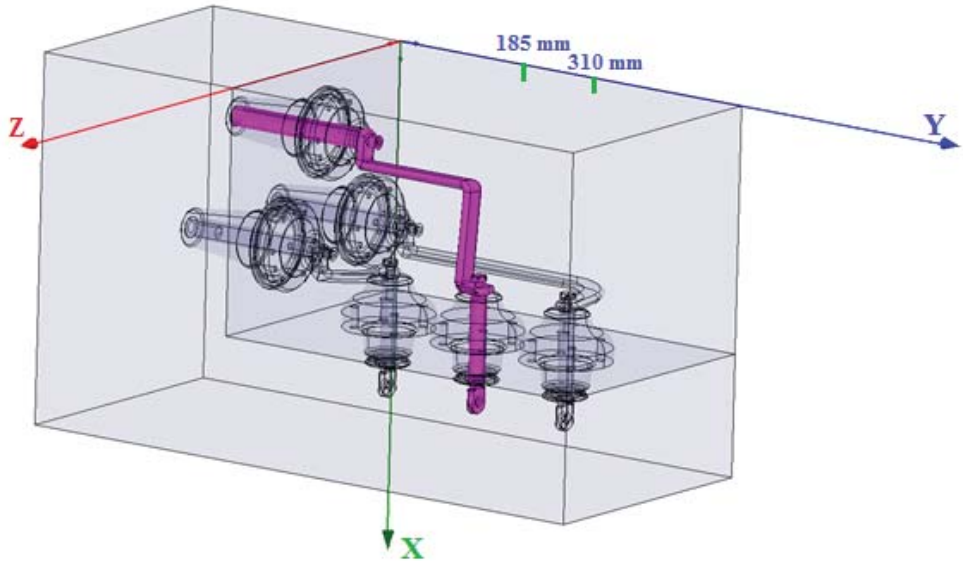

Fig. 13. Energised elements (magenta) in the feeder bay during the test of the insulation distances between phases

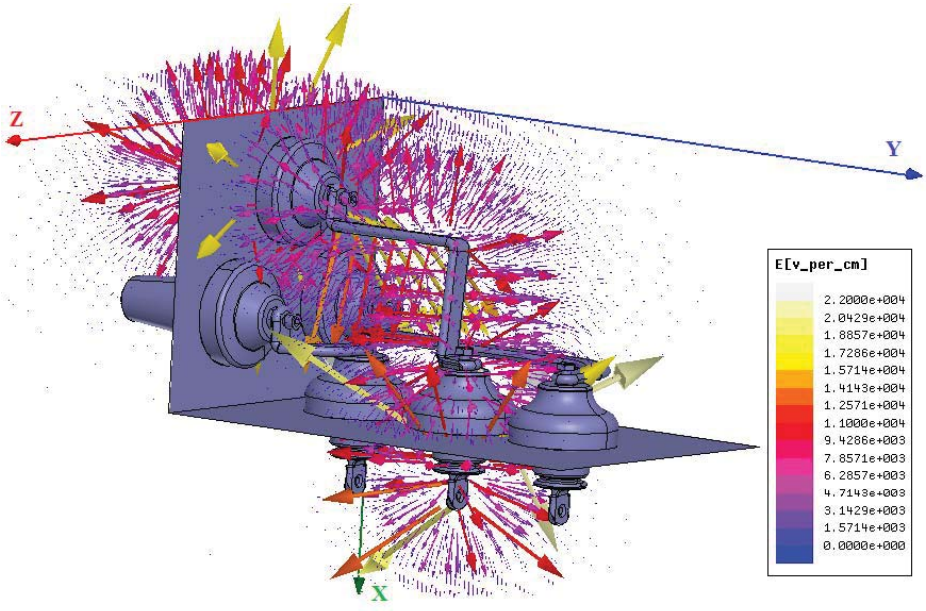

Fig. 14. Vector map of the electric field in the feeder bay (test of the insulation distances between phases)

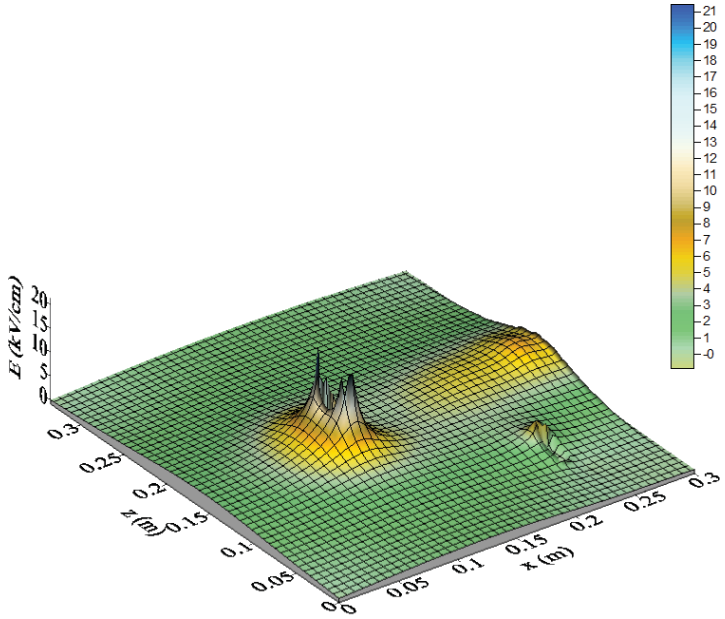

Fig. 15. Electric field distribution on the vertical plane (y = 185 mm) located between the vertical insulators in the feeder bay (test of the insulation distances between phases)

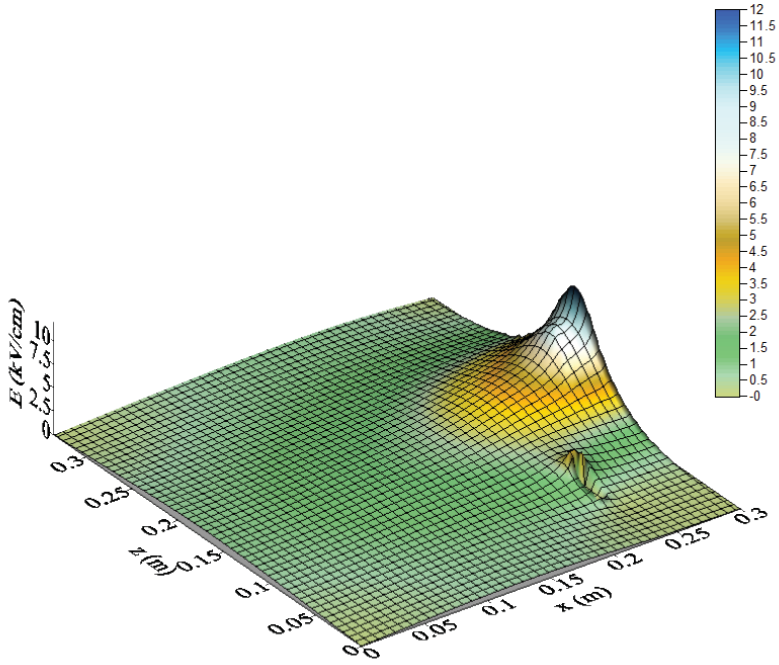

Fig. 16. Electric field distribution on the vertical plane (y = 310 mm) located between the insulator and the casing of the feeder bay (test of the insulation distances between phases)

7. COMPUTATIONAL RESULTS OF THE ELECTRIC FIELD DISTRIBUTION INSIDE THE BUSBAR COMPARTMENT

The electric field distribution inside the busbar compartment is analysed here. The overall dimensions of this compartment are 140 mm in *x* direction, 465 mm in *y* direction, and 1225 mm in z direction.

To start with, the computations concerning the test to earth were performed. As in the previous section, all conductors of the main circuit were connected to a single phase supply (Fig. 17).

The vector map of the electric field distribution in the region under consideration is shown in Figure 18. As could be predicted, the significant values of the electric field strength appear in the surroundings of the live conductors.

In Figures 19 and 20, the detailed electric field distribution on two selected vertical planes is shown, i.e. between the insulators (z = 350 mm) and between the insulators and the casing (z = 90 mm).

As in the feeder bay, the electric field strength does not exceed 28 kV/m on the above surfaces. Therefore, this value is about 2.5 times smaller than the electric withstand of the switchgear's general insulation.

The last electric field simulation concerns the test of the insulating distance between the busbar phases. In this test, one of the main circuit conductors was energised (Fig. 21) but the remaining ones and other metal elements were earthed.

The vector map of the electric field strength in the busbar compartment (for the above test) is shown in Figure 22. The electric field distributions on the planes where $z = 350$ mm and $y = 90$ mm are shown in Figures 23 and 24, respectively. In the first case, the electric field strength does not exceed 21 kV/m and in the second one this value is only 10 kV/m. The electric field strength of 21 kV/m is about 3.5 times smaller than the electric withstand of the SF_6 insulation.

The electric field simulation shown indicates that this switchgear compartment is also oversized and can be significantly reduced.

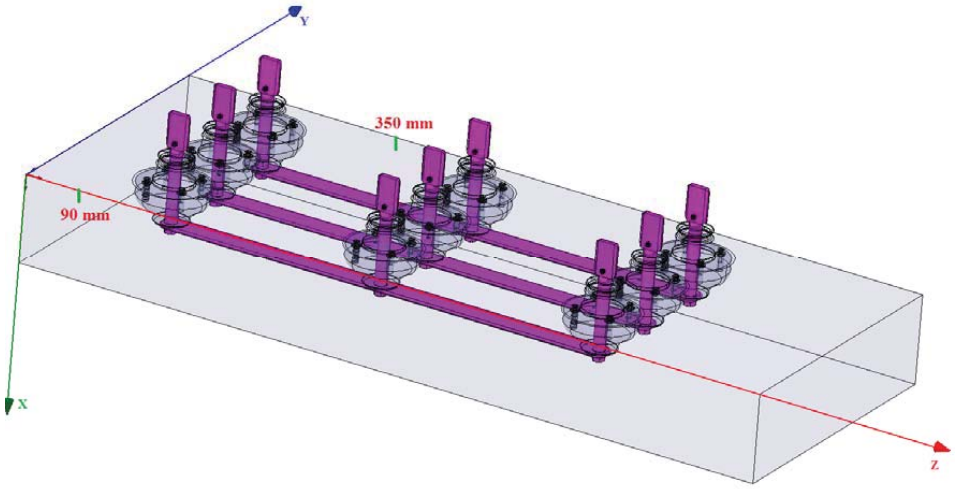

Fig. 17. Energised elements (magenta) in the busbar compartment during the test to earth

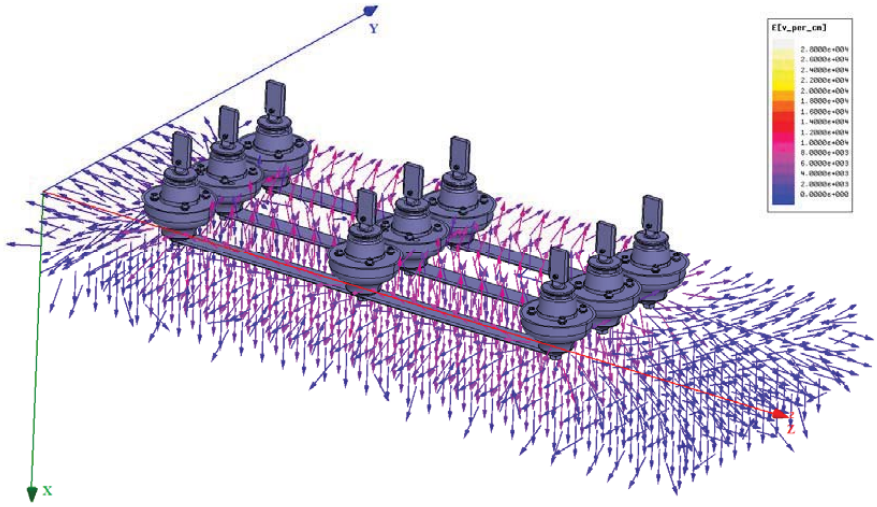

Fig. 18. Vector map of the electric field in the busbar compartment (test to earth conditions)

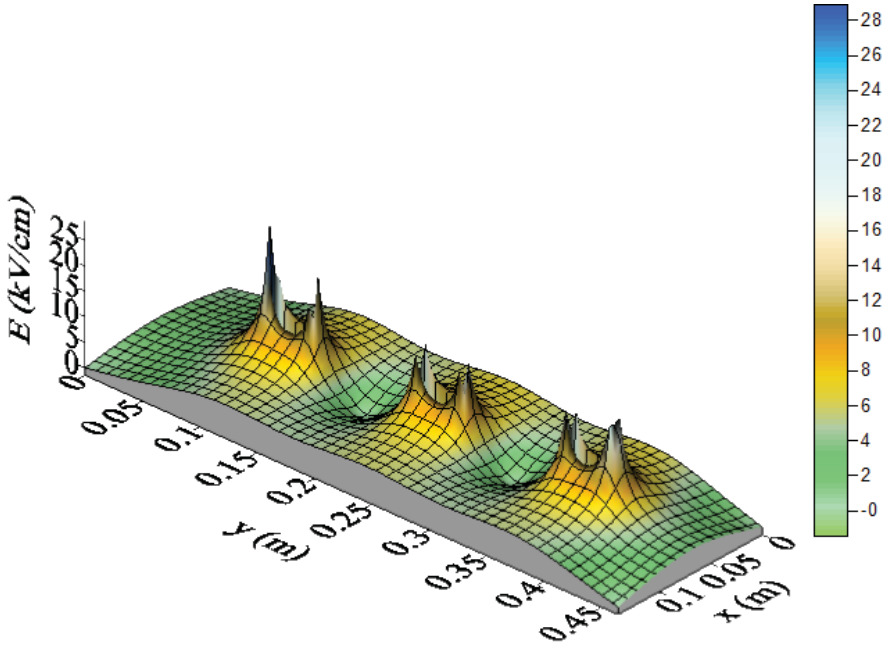

Fig. 19. Electric field distribution on a vertical plane (*z* = 350 mm) located between the insulators in the busbar compartment (test to earth)

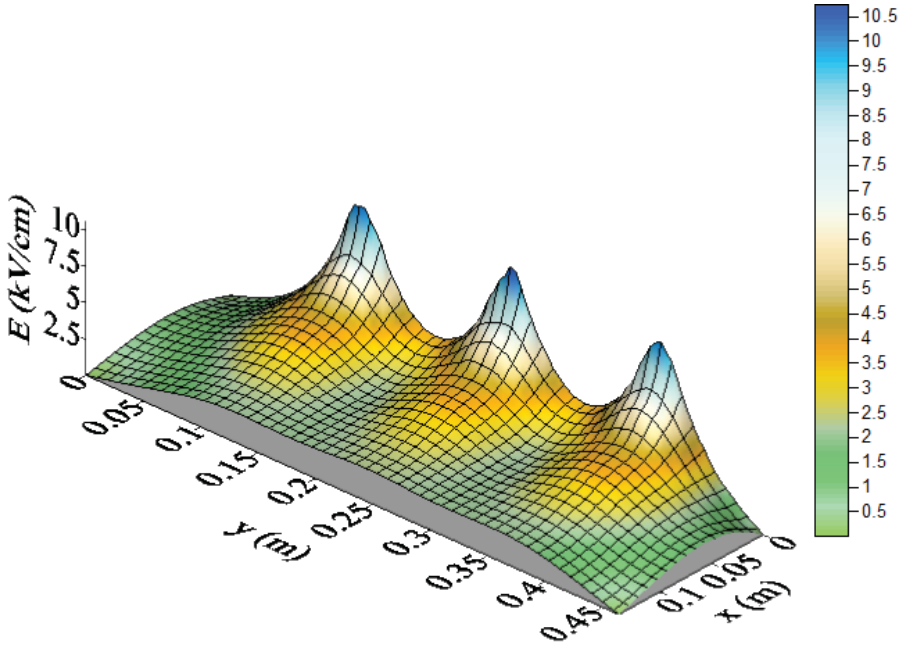

Fig. 20. Electric field distribution on a vertical plane (*z* = 90 mm) located between the insulators and wall of the busbar compartment (test to earth)

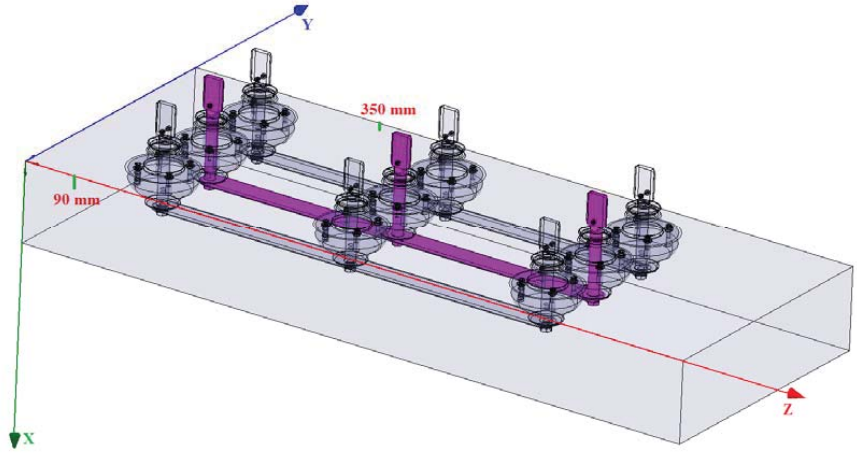

Fig. 21. Energised elements (magenta) in the busbar compartment during the test of the insulation distances between phases

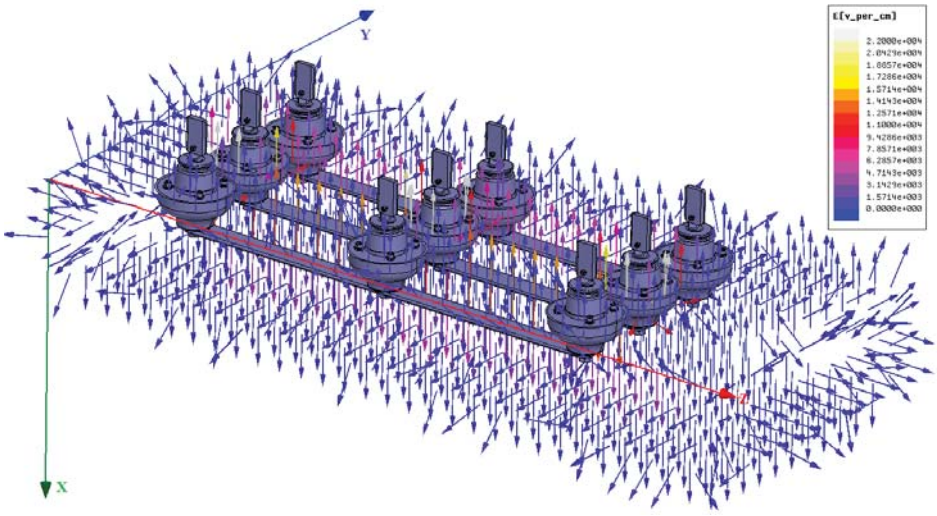

Fig. 22. Vector map of the electric field in the busbar compartment (test of the insulation distances between phases)

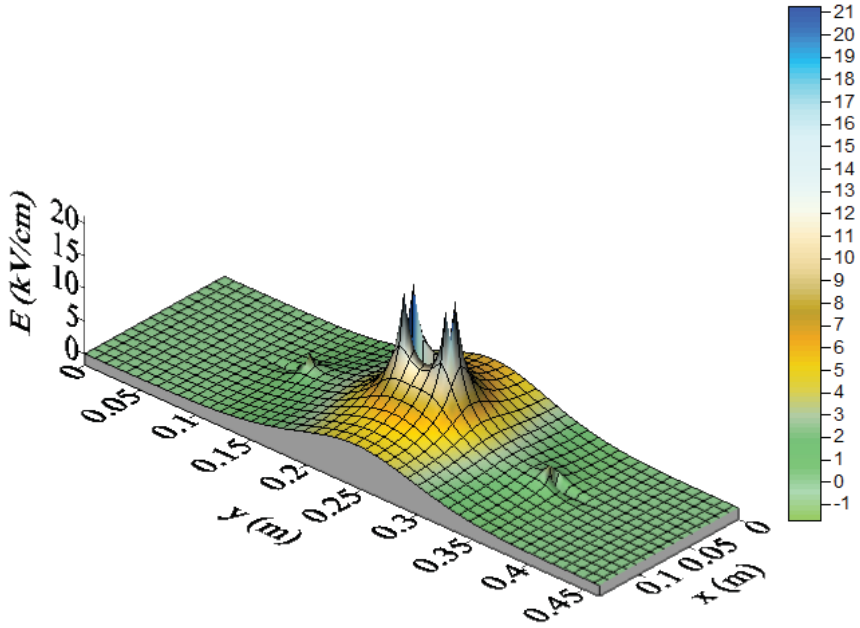

Fig. 23. Electric field distribution on the vertical plane (z = 350 mm) located between the insulators in the busbar compartment (test of the insulation distances between phases)

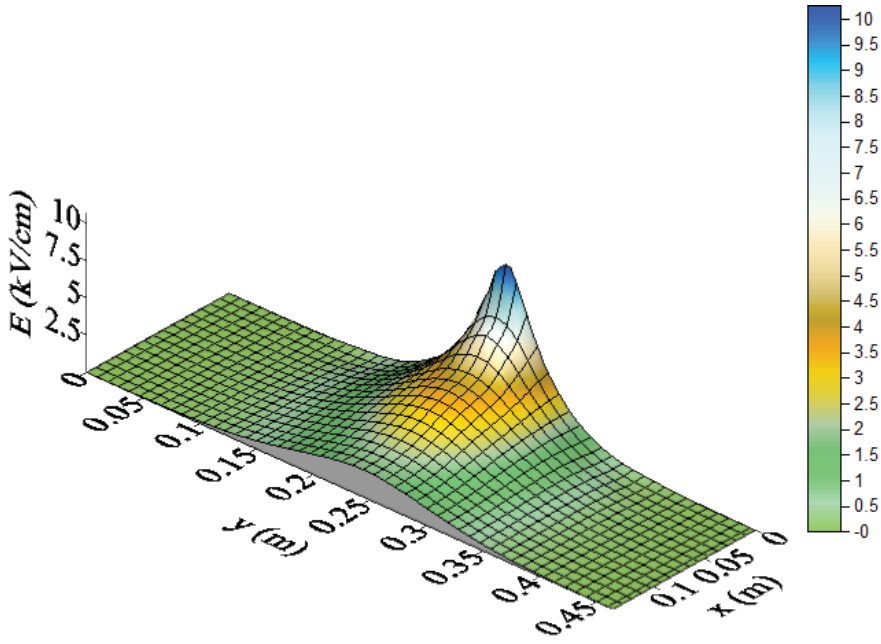

Fig. 24. Electric field distribution on the vertical plane (z = 90 mm) located between the insulators and wall of the busbar compartment (test of the insulation distances between phases)

7. CONCLUSIONS

The numerical simulation of the electric field inside the selected compartments of a 24 kV compact switchgear with SF_6 insulation has been described. This switchgear is currently in the process of being redesigned.

The conditions of the test to earth, as well as the phase to phase distance test, have been considered in computations.

The results obtained have enabled the maximum electric field strength in the feeder bay and in the busbar compartment to be determined.

The field analysis presented indicates that the switchgear compartments in question are oversized and their overall dimensions can be reduced.

If the factory decides to introduce appropriate changes and modifications of the switchgear geometry, similar electric field computations should be accomplished for the new switchgear dimensions. Such a procedure can be repeated several times to obtain the best switchgear version.

After the final numerical evaluation of the redesigned appliance, the switchgear prototype will be made in the factory. This prototype will be tested in the laboratory according to [3] (for the rated frequency and lightning impulse withstand voltages). The final results of these new investigations will be reported in the next article.

The computational approach proposed can be a useful tool that can improve and facilitate the designing and redesigning processes of gas-insulated switchgears and other electric power devices. Such an approach can shorten the designing process, can help to reduce the costs of device prototypes and can reduce the amount of laboratory tests needed.

LITERATURE

1. Krajewski W., Sibilski H., Wojciechowski R.: "Numerical modeling of the electric field in a 24 kV switchgear", *4th International Conference on High Voltage Engineering and Applications*, Poznań, 8–11 Sept. 2014, *IEEE Xplore,* added 09 February 2015, DOI: 10.1109/ICHVE.2014.7035390.
2. Krajewski W.: "Numerical evaluation of the electric field in a compact switchgear of medium voltage", *Prace Instytutu Elektrotechniki (Proceedings of Electrotechnical Institute)*, No. 267, 2014, pp. 35–47.
3. PN-EN 62271-200: 2012 "High-voltage switchgear and controlgear – Part 200: AC metal-enclosed switchgear and controlgear for rated voltages above 1 kV and up to and including 52 kV", *PKN (Polish Normalization Committee*).
4. http://www.ansys.com/Products/Electronics/ANSYS-Maxwell, Access : 13.06.2016.
5. Zienkiewicz O.C.: "The Finite Element in Engineering Science", McGraw-Hill, New York, 1971.
6. Kuffel E., Kuffel J., Zaengl W.S.: "High Voltage Engineering Fundamentals", Newnes, 2000.
7. Fotyma M., Życzyńska B.: "Withstand of sulphur hexafluoride in different electrode configurations", *Prace Instytutu Elektrotechniki (Proceedings of Electrotechnical Institute)*, No. 49, 1966, pp. 91–109 (in Polish).
8. Brebbia C.A.: "The Boundary Element Method for Engineers", Pentech Press, London, 1978.
9. Singer H., Steinbigler H., Weiss P.: "A charge simulation method for the calculation of high voltage fields", *IEEE Trans. on Power Apparatus and Systems*, Vol. 93, 1974, pp. 1660 – 1668.

10. Salon S.: "The hybrid finite element – boundary element method in electromagnetics", *IEEE Trans. on Magnetics*, Vol. 22, 1985, pp. 1829–1834.
11. Krajewski W.: "Boundary and line elements in the analysis of selected EMC problems of low frequency", *Prace Instytutu Elektrotechniki (Proceedings of Electrotechnical Institute)*, No. 224, 2005, (Monograph in Polish).
12. Krajewski W.: "Numerical modelling of the electric field in HV substations", *IEE Proc. Sci. Meas. Technol*., Vol. 151, No. 4, 2004, pp. 267–272.
13. Krajewski W.: "BEM analysis of 3D EMC problem with consideration of eddy-current effects", *IEE Proc. Sci. Measur. Technol.*, Vol. 153, No. 3, 2006, pp. 101–107.
14. Trkulja B., Štih Ž.: "Computation of electric fields inside large substations," *IEEE Trans. on Power Delivery*, Vol. 24, No. 4, 2009, pp. 1898–1902.
15. Ranković A., Savić M.S.: "Generalized charge simulation method for the calculation of the electric field in high voltage substations", *Electrical Engineering*, Vol. 92, No. 2, July 2010, pp. 69–77.
16. Shaalan E.M., Ghania S.M., Ward S.A.: "Analysis and measurement of electric field exposure inside a 500/220 kV air insulated substation", *Journal of Electrical Engineering*, Vol. 12, Issue 2, 2012, pp. 77–84.
17. Metwally I.A.: "Reduction of electric-field intensification inside GIS by controlling spacer material and design", *Journal of Electrostatics*, Vol. 70, 2012, pp. 217–224.

Accepted for publication 17.05.2017

MINIATURYZACJA KOMPAKTOWEJ ROZDZIELNICY ŚREDNIEGO NAPIĘCIA

Wojciech KRAJEWSKI

STRESZCZENIE *Miniaturyzacja rozdzielnic kompaktowych wiąże się z oszczędnością materiałów, co, poza zmniejszeniem gabarytów, przyczynia się do obniżenia ich ceny rynkowej. To z kolei zwiększa konkurencyjność i atrakcyjność rynkową produktu, przekładając się na wolumen sprzedaży. Jest to zatem korzystne zarówno dla producentów, jak i odbiorców. Niemniej jednak, oszczędność materiałów nie może pogarszać jakości produktu finalnego. W artykule przedstawiono pewne aspekty miniaturyzacji rozdzielnicy kompaktowej 24 kV, produkowanej przez krajową firmę ZPUE S.A. Biuro konstrukcyjne tej spółki zaproponowało usunięcie niektórych elementów wcześniej produkowanego urządzenia. Pozbyto się zbędnych ścianek działowych, jak i niektórych elementów obudowy zewnętrznej, zmniejszając w ten sposób wagę, gabaryty i zużycie materiałów. W niniejszym artykule przeanalizowano dalszą możliwość zmniejszenia wymiarów gabarytowych rozdzielnicy. W tym celu przeprowadzono analizę numeryczną pola elektrycznego wewnątrz wybranych jej przedziałów. Zastosowano w tym celu oprogramowanie Maxwell 3D firmy Ansys, bazujące na metodzie elementów skończonych.*

Słowa kluczowe: *metoda elementów skończonych, miniaturyzacja, pole elektryczne, rozdzielnica kompaktowa, wytrzymałość elektryczna*

Assoc. Professor Wojciech KRAJEWSKI received the M.Sc. and Ph.D. degrees in electrical engineering from the Warsaw Technical University in 1977 and 1984, respectively. He received the D.Sc. degree (habilitation) from the Electrotechnical Institute, Warsaw, Poland, in 2007, in technical science. He is with the above Institute since 1981 up to now. He works on numerical modelling of electromagnetic fields in electrical machines and devices as well as in the human environment and human organism. He is an author and co-author of computer software packages based on the boundary element method and over fifty scientific papers published in domestic and international journals. Assoc. Professor Wojciech Krajewski is a member of the Association of Polish Electricians (SEP) and the Institution of Engineering and Technology (IET).